Journal of Assisted Reproduction and Genetics (2019) 36:349–359
https://doi.org/10.1007/s10815-018-1353-8

FERTILITY PRESERVATION

# Evaluation of Z-VAD-FMK as an anti-apoptotic drug to prevent granulosa cell apoptosis and follicular death after human ovarian tissue transplantation

Maïté Fransolet[1] · Laure Noël[1,2] · Laurie Henry[2] · Soraya Labied[2] · Silvia Blacher[1] · Michelle Nisolle[1,2] · Carine Munaut[1]

Received: 26 July 2018 / Accepted: 19 October 2018 / Published online: 3 November 2018


## Abstract

**Purpose** To evaluate the efficiency of ovarian tissue treatment with Z-VAD-FMK, a broad-spectrum caspase inhibitor, to prevent follicle loss induced by ischemia/reperfusion injury after transplantation.

**Methods** In vitro, granulosa cells were exposed to hypoxic conditions, reproducing early ischemia after ovarian tissue transplantation, and treated with Z-VAD-FMK (50 μM). In vivo, cryopreserved human ovarian fragments ($n = 39$) were embedded in a collagen matrix containing or not Z-VAD-FMK (50 μM) and xenotransplanted on SCID mice ovaries for 3 days or 3 weeks.

**Results** In vitro, Z-VAD-FMK maintained the metabolic activity of granulosa cells, reduced HGL5 cell death, and decreased PARP cleavage. In vivo, no improvement of follicular pool and global tissue preservation was observed with Z-VAD-FMK in ovarian tissue recovered 3-days post-grafting. Conversely, after 3 weeks of transplantation, the primary follicular density was higher in fragments treated with Z-VAD-FMK. This improvement was associated with a decreased percentage of apoptosis in the tissue.

**Conclusions** In situ administration of Z-VAD-FMK slightly improves primary follicular preservation and reduces global apoptosis after 3 weeks of transplantation. Data presented herein will help to guide further researches towards a combined approach targeting multiple cell death pathways, angiogenesis stimulation, and follicular recruitment inhibition.

**Keywords** Fertility preservation · Apoptosis · Granulosa cells · Ovarian tissue transplantation · Z-VAD-FMK

## Introduction

Anticancer therapies gave some long-term side effects and can place young women at risk for premature ovarian failure [1]. Therefore, multiple approaches have been developed to preserve and restore female fertility [2]. Ovarian tissue cryopreservation is commonly offered when cancer therapy cannot be delayed. Nowadays, it represents the only option that demonstrated its effectiveness to preserve fertility of prepubertal female patients [3]. Currently, more than 130 live births were reported as a result of frozen-thawed ovarian tissue autotransplantation and the pregnancy rate is about 30% [4, 5]. The successful outcome of this approach strongly depends on the angiogenic process. Indeed, blood reperfusion is not achieved immediately in small-grafted ovarian fragments. The hypoxic period, lasting for 3 to 5 days before revascularization [6], results in ischemia/reperfusion (I/R) injury by oxygen-derived free radicals responsible for follicular loss [7] and stroma integrity damages [8, 9]. In order to lengthen the reproductive lifespan of the graft, it is essential to improve the ovarian tissue survival early after transplantation.

Numerous approaches have already been elaborated to minimize ischemic injury [10–14] and to improve the neovascularization process of the ovarian tissue. However, in studies using cortical tissue from human or species with close ovarian histology, a faster angiogenesis was not necessarily associated to a better preantral follicle preservation after grafting [15–18].

In I/R injury, apoptosis is also responsible of cell death [19]. In rodent ovaries, follicles were identified to be apoptotic soon

**Electronic supplementary material** The online version of this article (https://doi.org/10.1007/s10815-018-1353-8) contains supplementary material, which is available to authorized users.

✉ Carine Munaut
c.munaut@ulg.ac.be

[1] Laboratory of Tumor and Developmental Biology, GIGA-R, University of Liège, Tour de Pathologie (B23), Avenue Hippocrate, 13, Sart Tilman, B-4000 Liège, Belgium

[2] Department of Gynecology and Obstetrics, CPMA, University of Liège, CHR de la Citadelle, Boulevard du 12ième de Ligne, 1, B-4000 Liège, Belgium

after transplantation [20, 21]. Apoptosis is a programmed cell death displaying specific features that involves activation of caspases, which are the executioner proteins of apoptosis [22]. Caspases inhibition could therefore be an attractive strategy to prevent follicular apoptosis.

Several studies demonstrated the effectiveness of caspase inhibitors to prevent apoptosis and I/R injury in several tissues exposed to ischemia such as myocardium [23], brain [24], liver [25], muscle [26], intestine [27], and pancreas [28]. The benzyloxycarbonyl-Val-Ala-Asp-fluoromethyl ketone (Z-VAD-FMK) is a cell permeable broad-spectrum caspase inhibitor with no cytotoxic effects that irreversibly binds to the catalytic site of caspases [29]. Recently, we demonstrated that Z-VAD-FMK treatment prior to ovarian tissue cryopreservation improves primordial follicular quality and global tissue survival [30]. In mice ovaries, a higher number of proliferative cells and a reduction of the delay to resume estrous cycle were observed after grafting when Z-VAD-FMK was included in vitrification and thawing solutions [31].

Altogether, these results suggest that Z-VAD-FMK could improve the preservation of biological material used in organ transplantation, such as ovarian fragments, after grafting. Nowadays, no data are available concerning the effect of Z-VAD-FMK on follicular pool preservation and the overall survival of human ovarian grafts.

In the current study, we evaluated the effect of Z-VAD-FMK in vitro on human granulosa cell death caused by hypoxia and in vivo after human ovarian tissue transplantation.

## Materials and methods

### Primary human granulosa cell isolation

Primary human granulosa cells (hGC) were isolated from follicular fluid collected from patients undergoing oocyte retrievals at the Center of AMP in Liège (CPMA, CHR Citadelle), based on a protocol adapted from Shi et al. [32]. After oocyte isolation, pooled follicular fluid was centrifuged for 10 min at 400 g. After removing the supernatant, the pellet was resuspended in 2 ml of HBSS solution (Gibco) containing collagenase (0.28 mg/ml, Sigma-Aldrich), hyaluronidase (0.23 mg/ml, LifeGlobal Group), and bovine serum albumin (BSA, 0.8 mg/ml, Acros Organics) and shaked at 225 rpm for 20 min at 37 °C. Cells were then layered on 7 ml Ficoll-Paque (GE Healthcare) and centrifuged for 20 min at 600 g. Before magnetic cell sorting (MACS), the collected cell layer was washed twice in Dulbecco's modified Eagle's medium/F-12 (Gibco), and the number of viable cells was determined by using trypan blue. Cells were resuspended in 80 μl recommended buffer per $10^7$ cells. Monoclonal mouse anti-human CD45 antibody conjugated with microbeads (Miltenyi Biotec) was added to the cellular suspension (20 μl per $10^7$ total cells) and incubated at 4 °C for 15 min. After that, 10 μl of monoclonal mouse anti-human CD45 antibody conjugated to FITC recognizing another epitope was added and incubated at 4 °C for 5 min. Finally, cells were washed and loaded on top of the MS separation column placed in the magnetic field. The CD45 negative cells flowed through the column and were collected. The purity percent of isolated cells was evaluated by flow cytometry at a FACSCanto II (BD Biosciences) and it exceeded 96% for CD45-negative fraction (primary hGC).

### Cell culture and treatment

The HGL5 cell line and primary hGC were maintained in Dulbecco's modified Eagle's medium/F-12, supplemented with 10% heat-inactivated fetal bovine serum, 100 IU/ml penicillin-100 μg/ml streptomycin and, for hGC, 1% ITS (6.25 μg/ml insulin, 6.25 μg/ml transferrin, 6.25 selenium μg/ml). Culture reagents were purchased from Gibco. To expose cells to hypoxic and nutrient deficient conditions, cells were treated with cobalt chloride ($CoCl_2$) at 500 μM and maintained in DMEM/F12 containing or not FBS for 24 h. Z-VAD-FMK was added at a concentration of 50 μM (R&D Systems).

### WST-1 assay

The cell metabolic activity was estimated using a WST1 assay (Roche) as previously described [33]. Cell metabolic activity was calculated using the following equation: $(OD_{450} - OD_{620})_{test} - (OD_{450} - OD_{620})_{blank}$. Experiments were repeated at least four times.

### Flow cytometry

Granulosa cell apoptosis was analyzed by flow cytometry after annexin V-FITC and propidium iodide double staining using a BD Pharmingen™ Annexin V FITC apoptosis detection kit (BD Pharmingen) as previously described [33]. HGL5 and primary granulosa cells were seeded in 6 cm petri dishes at a density of $6.0 \times 10^5$ and $2.0 \times 10^5$ cells, respectively. Experiments were repeated at least three times.

### Western blot

Whole cell extracts were prepared as previously described [33]. Proteins were detected by incubation with a polyclonal anti-PARP antibody (#9542, Cell Signaling) or anti-Actin (A2066, Sigma) followed by 1-h incubation with horseradish peroxidase-conjugated swine anti-rabbit secondary antibody (P0399, Dako) and ECL (PerkinElmer Life Sciences) revelation in LAS4000 imager (Fujifilm). The relative intensity of full-length and cleaved PARP protein was measured by Quantity One® Software and normalized by the amount of actin (loading control). Relative density value for each condition was

expressed as fold induction by dividing the relative density value of each sample by the relative density value of the control.

## Collection, preparation, freezing, and thawing process of ovarian tissue

Human ovarian cortex was obtained from a 35-year-old woman undergoing ovarian tissue cryopreservation (CPMA, CHR Citadelle) before gonadotoxic treatments. The patient signed informed consent for research use of her ovarian fragments. After surgery, ovaries were kept at 4 °C until processing in Leibovitz L-15 medium (Lonza) supplemented with 10% human serum albumin (Irvine Scientific). In the laboratory, the medulla was removed and the cortex was cut into strips (5 × 2.5 × 1 mm) before equilibration during 30 min at 4 °C in cryopreservative medium containing Leibovitz L-15 medium supplemented with 10% human serum albumin, 10% dimethylsulfoxide (1.5 M) (Sigma-Aldrich), and 0.1 M sucrose. Ovarian biopsies were cooled in a programmable Planner freezer (Planner Kryo 360-3.3) in cryovial tubes (Simport) as previously described [34].

On the day of the transplantation procedure, ovarian fragments were thawed as previously described [14].

## Ovarian transplant encapsulation

Cortical biopsies of 2.5 × 2.5 × 1 mm were embedded in a three-dimensional collagen matrix, as previously described [14]. Z-VAD-FMK was included in the collagen of treated group at a concentration of 50 μM.

## Mouse transplantation and sacrifice

Eight-week-old severe combined immunodeficient (SCID, $n = 20$) female mice were purchased from Charles River Laboratory. Fifty-four frozen-thawed human ovarian fragments were randomly assigned to five groups. Fourteen pieces were used as pregraft controls (frozen-thawed, $n = 14$) and the other ones were transplanted ($n = 10$ fragments per group) (Online Resource 1). One encapsulated ovarian biopsy was stitched on each ovaries of mice under isoflurane (Abbott) anesthesia with a 7–0 Prolene suture.

Animals were euthanized by cervical dislocation 3 days or 3 weeks after grafting. For hypoxic area detection, mice were injected intraperitoneally with 100 mg/kg of pimonidazole (Hydroxyprobe-1, Chemicon) 2 hours before ovarian tissue recovery. For the functional vascular network analysis 3 days after transplantation, mice received intravenously 200 μL of dextran/FITC solution (2.5 mg/mL in PBS; Sigma-Aldrich) 3 min before sacrifice.

## Histological analyses

Grafts were recovered, fixed in 4% formaldehyde, embedded in paraffin, and cut into 5-μm-thick serial sections for histological assessment.

Apoptotic cells were identified by TUNEL staining using ApopTag® Plus Fluorescein in situ Apoptosis Detection Kit (S7111, Chemicon), according to the manufacturer's instructions. Follicles were considered positive for TUNEL if the oocyte was stained and/or if at least 50% of the granulosa cells were stained.

After antigen retrieval and blocking of unspecific binding sites, cell proliferation and hypoxia were immunolabeled by incubating histological sections with their respective primary antibodies and their appropriate secondary antibodies (Online Resource 2). The 3,3′-diaminobenzidine substrate (K3468, Dako) allowed the visualization of the staining and the sections were counterstained with hematoxylin. To detect the functional vascular network, immunostaining was performed in one step as previously described [35]. Negative control slides were performed by replacing the primary antibody with phosphate-buffered saline (PBS). Slides were digitized as previously described [35].

Every sixth section of each graft was stained with hematoxylin and eosin (H&E) and at least eight H&E sections per transplant were analyzed. Follicles were quantified manually and, to avoid double counting, only follicles with a visible nucleus were taken into account. Follicles were then classified according to their maturity (Online Resource 3). Follicular densities (number/mm$^2$) were calculated from the graft surface analyzed by the NDP.view software (Olympus).

Proliferating cells, stained in brown color, were automatically quantified using the image analysis toolbox of MATLAB 9.0.0.341360 (R2016a) (MathWorks, Inc.). Because cell detection was mainly based on color segmentation, contrast was first enhanced by determining the excess of the red component (two times red value minus blue value minus green value). Then, based on the enhanced red component of the resulting color image, binary images of the cells (i.e., pixels belonging to cells were assigned an intensity of 1, whereas background pixels were assigned an intensity of 0) were obtained using an automatic entropy threshold. To eliminate small artifacts, morphological filters were applied on the resultant images. Binary images of the total tissue sections were obtained by applying an appropriate threshold to the blue component of the images. Lastly, cell density was defined as the area occupied by cells divided by the total area of the section.

Apoptotic cells were stained with green color. They were detected using the same methodology on the green component of the color image.

## Statistical analysis

All quantitative results are expressed as the mean ± S.E.M. of at least three independent experiments (see above and results). One-

way ANOVA and Kruskal-Wallis tests were applied for exploratory data analyses and the Mann-Whithney *U* test was applied for non-parametric independent two-group comparisons. Values of at least $P < 0.05$ were considered statistically significant. All tests were performed using GraphPad Prism 5.0 software (La Jolla).

## Results

### Z-VAD-FMK in vitro on granulosa cells

Cells were treated with cobalt chloride ($CoCl_2$) to mimic hypoxia. WST1 assays indicated that $CoCl_2$ markedly decreases the metabolic activity of the HGL5 and primary hGC with or without serum. Co-treatment with Z-VAD-FMK partially restored the metabolic activity of HGL5 cells in absence of serum (Fig. 1a) but not in primary cells (Fig. 1d). Flow cytometry analyses after apoptosis staining confirmed these results (Fig. 1b and e). HGL5 cells treated with $CoCl_2$ and Z-VAD-FMK displayed a higher number of viable cells. No difference between conditions was observed in co-treated primary cells.

**Fig. 2** Histological analyses and follicular pool evaluation of ovarian tissue. Representative H&E staining images of ovarian cortical sections from frozen-thawed fragments prior to transplantation (**a**), control (**b** and **e**, 3 days and 3 weeks respectively), and Z-VAD-FMK-treated grafts (**c** and **f**, 3 days and 3 weeks respectively). Quantification of primordial, primary, and secondary (or more) follicle density in frozen-thawed fragments and ovarian grafts 3 days (**d**) or 3 weeks (**g**) after transplantation in SCID mice. Every sixth section of each graft ($n = 9$ to 10) was stained with hematoxylin and eosin (H&E) and at least eight H&E sections per transplant were analyzed for follicular quantification. Morphologically abnormal follicle is identified by a plain arrow. ▸ Indicates vessels. Scale bar: 500 μM. For follicular quantification, the results are presented as box-and-whisker plots, illustrating the median (central bar), 25th and 75th percentiles (bottom and top of the box) and minimum and maximum values (lower and upper bars). * $P < 0.05$ and ** $P < 0.01$

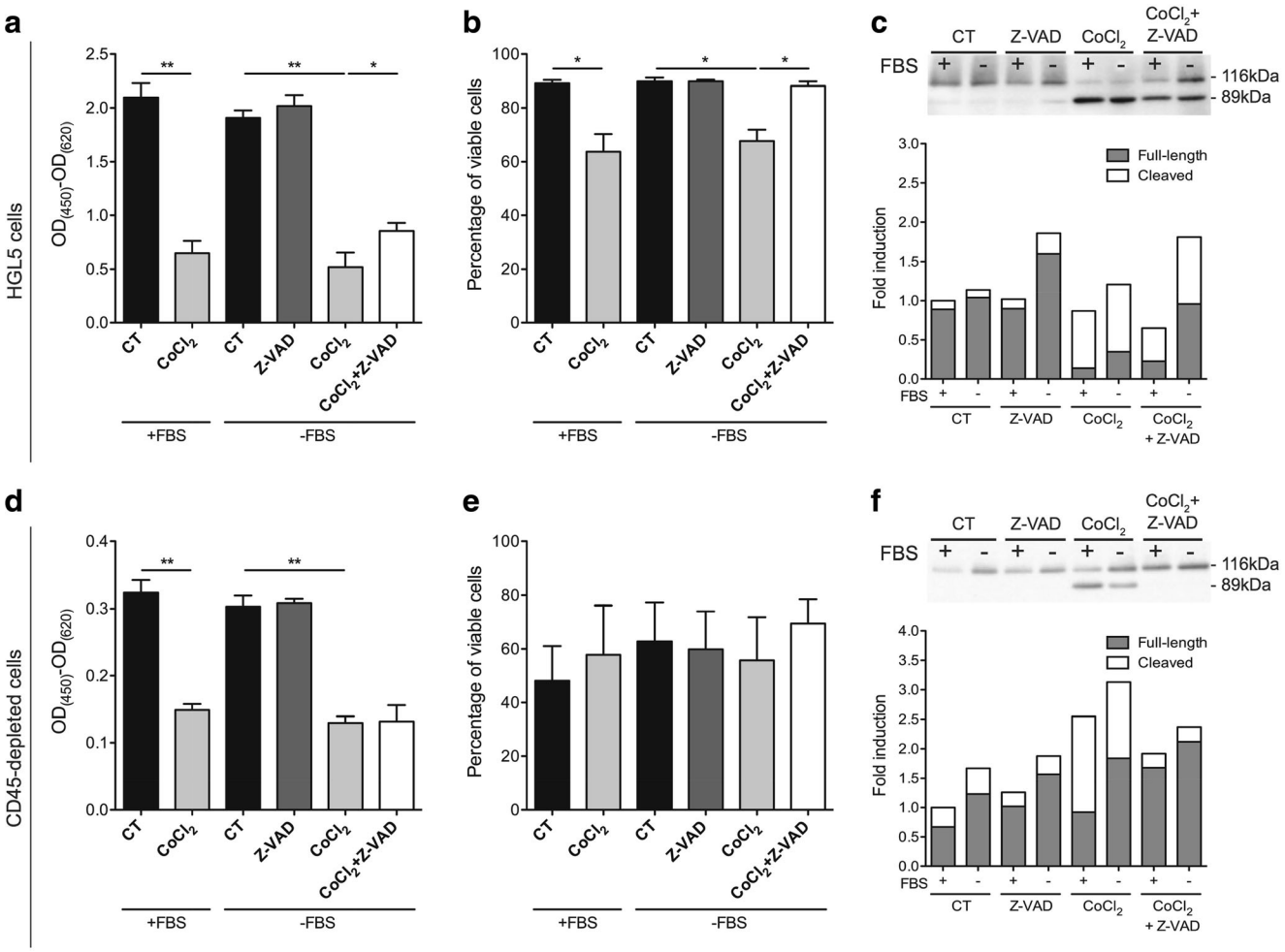


**Fig. 1** Granulosa cell metabolic activity, viability, and PARP cleavage under hypoxic conditions (HGL5, **a**–**c**; primary hGC (CD45-depleted cells), **d**–**f**). Evaluation of the metabolic activity measured by WST1-1 assay (**a** and **d**). Percentage of viable cells detected by flow cytometry analyses (**b** and **e**). Data are expressed as mean ± S.E.M. of at least three independent experiments. Representative images of western blot highlighting the expression of PARP and quantitative analyses associated (**c** and **f**). The graphs represent densitometric analysis of bands with the relative density value for each condition expressed as fold induction by dividing the relative density value of each sample by the relative density value of the control. Data are expressed as mean of three independent experiments. * $P < 0.05$ and ** $P < 0.01$

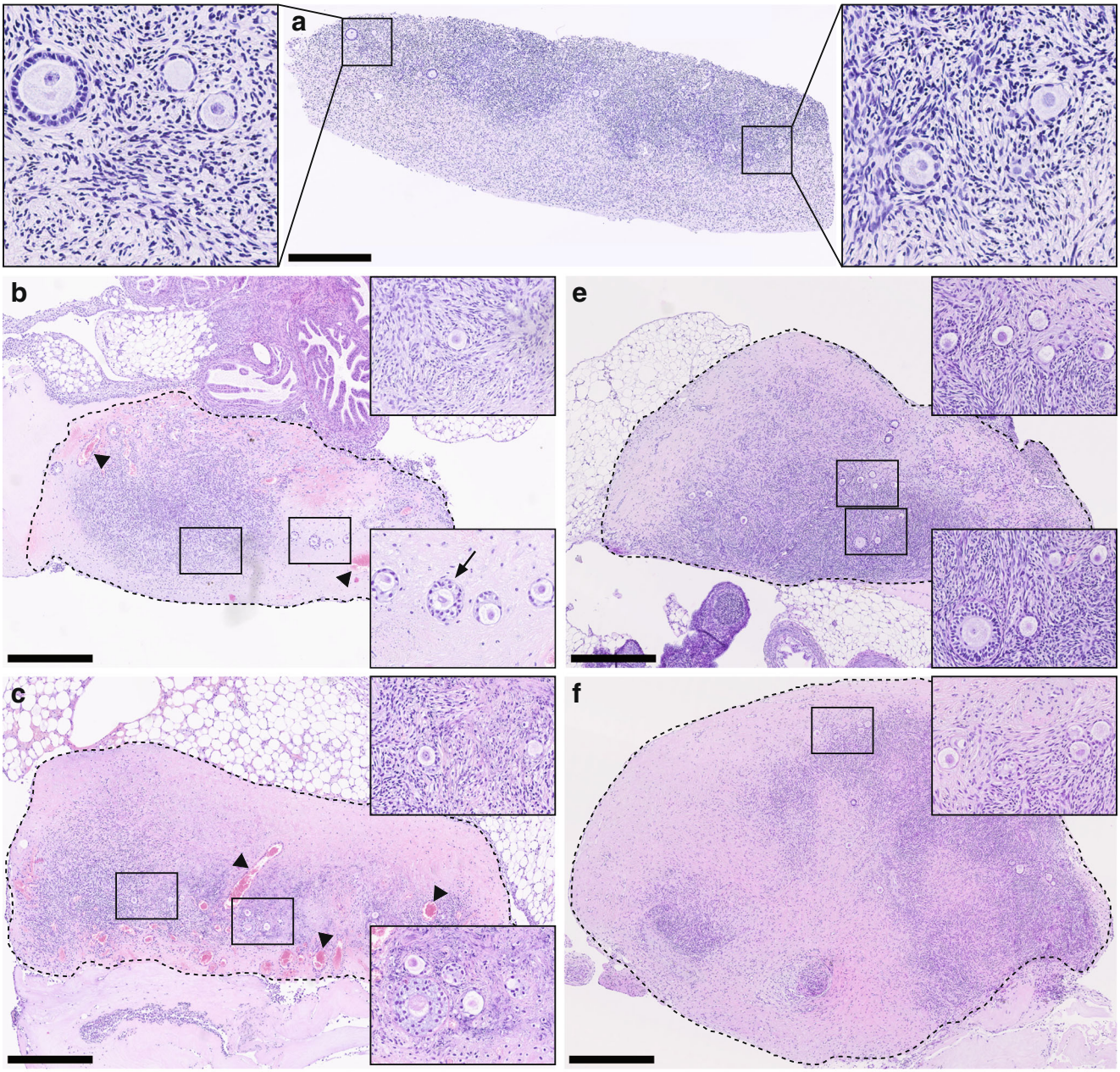
a
b
c
e
f

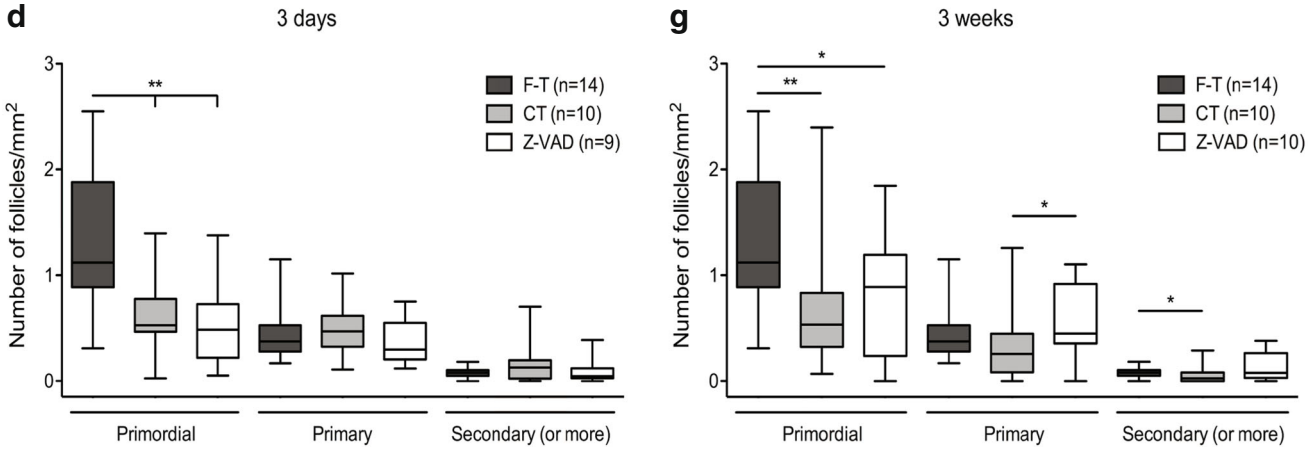
d
3 days
Number of follicles/mm2
F-T (n=14)
CT (n=10)
Z-VAD (n=9)
Primordial
Primary
Secondary (or more)
g
3 weeks
Number of follicles/mm2
F-T (n=14)
CT (n=10)
Z-VAD (n=10)
Primordial
Primary
Secondary (or more)

As one of the main targets of caspase-3, Poly (ADP-ribose) polymerase (PARP) expression was evaluated by western blot and revealed that $CoCl_2$ treatment increased significantly the level of cleaved-PARP in HGL5 cells as well as in primary hGC CD45-depleted granulosa cells, with or without serum. Co-treatment with Z-VAD-FMK reduced PARP cleavage, mostly in hGC CD45-depleted cells (Fig. 1c and f).

## Z-VAD-FMK in vivo on grafted ovarian fragments

**Morphological analysis and follicular pool assessment** Except one piece treated during 3 days with Z-VAD-FMK, all the ovarian fragments were recovered after xenograft in SCID mice (Online Resource 1). The morphology of frozen-thawed fragments was similar to fresh tissue. They presented a dense stroma with normal follicles located in the cortex (Fig. 2a). Representative images confirmed the important vascular remodeling previously shown 3 days after transplantation [35]. In these fragments, follicles in the cortical region looked healthy but some of those found in fibrotic areas presented abnormal morphological features, regardless of the treatment (Fig. 2b and c). In comparison with frozen-thawed fragments from the same patient, primordial follicular density was largely decreased after grafting whereas the densities of more mature follicles were the same before and after grafting. Z-VAD-FMK treatment did not affect follicular density (Fig. 2d). When recovered 3 weeks after the transplantation, fragments revealed an unaltered morphology with a major part of morphologically normal follicles in the cortical zone (Fig. 2e and f). The decrease of primordial follicle density observed 3 days after transplantation was confirmed by the follicular analysis at 3-weeks post-grafting. Moreover, a reduction of secondary follicle density was evidenced in the fragments from the control group transplanted during 3 weeks in comparison with the pregraft control. No difference was observed between the two grafted groups concerning the density of primordial and secondary follicles but primary follicles were better preserved with Z-VAD-FMK (Fig. 2g). We also evidenced that 3 weeks after grafting, the mean densities of the different follicular stages were the same than those observed 3 days after grafting.

**Apoptosis** TUNEL-positive follicles (Fig. 3a–c) were almost exclusively detected 3 days after grafting in the two experimental groups (Fig. 3g). In these follicles, only oocytes were positive for the TUNEL staining. In some H&E sections, regardless of the treatment, follicles with pyknotic oocytes (darkly eosinophilic) were observed. However, some of them were negative for the TUNEL staining (Fig. 3d). In the two experimental groups, follicles were the only cellular structures present in area with high degree of fibrosis and they were positive (Fig. 3e) or negative (Fig. 3f) for the TUNEL staining.

The number of TUNEL-negative and positive follicles were counted and no difference was detected between control and Z-VAD-FMK-treated grafts after 3 days or 3 weeks of transplantation (Fig. 3g). In ovarian tissue recovered 3 weeks after xenograft, only one follicle in the control group displayed TUNEL-positive staining.

Quantification of the global stromal and follicular apoptosis revealed that the percentage of apoptosis was lower after 3 weeks of transplantation than after 3 days (Fig. 3h). These results were consistent with those from the percentage of apoptotic follicles (Fig. 3g). The apoptosis detected throughout the ovarian tissue recovered after 3 weeks of transplantation was reduced by Z-VAD-FMK treatment as compared to the control (Fig. 3h).

**Cellular proliferation** Three days after transplantation, proliferative cells were often located at the external boundary of the fragment. Some granulosa cells were stained, indicating a follicular activity (Fig. 4a and b). Quantification of the proliferative cells revealed no difference between the two groups (Fig. 4c). In ovarian tissue recovered 3-weeks post-transplantation, proliferative cells were disseminated throughout the fragment and some granulosa cells were still proliferative (Fig. 4d and e). Z-VAD-FMK did not affect cell proliferation (Fig. 4f). The mean number of proliferative cells detected on the ovarian tissue grafted during 3 days is halved after 3 weeks of transplantation.

**Hypoxia** Three-days post-grafting, hypoxic areas were mainly localized in the area of the fragment devoted of proliferative cells (Fig. 4g) or distributed throughout the fragment (Fig. 4h). The overall hypoxia of the tissue was not affected by Z-VAD-FMK treatment (Fig. 4i). In fragments recovered after 3 weeks, pimonidazole staining was much more reduced and was not different between the controls or Z-VAD-FMK-treated fragments (Fig. 4j–l). The percentage of pimonidazole positive staining was five times lower in the long-term experiments than in the short-term ones indicating the correct reperfusion of the grafts.

**Revascularization and functional vascular network** At short term after grafting, functional vessels were located at the external boundary of the fragment (Fig. 4m and n) mostly corresponding to the proliferative area and to the opposite of the hypoxic zones. Analyses of the staining revealed that 70% of the control and 56% of the Z-VAD-FMK-treated transplants were perfused. Among these fragments, the mean number of functional vessels was quantified and the ovarian tissue neoangiogenesis was the same in the two groups (Fig. 4o).

## Discussion

Given the previous encouraging results obtained with the Z-VAD-FMK [30, 31], we investigated for the first time its effect in vitro on human granulosa cells and on grafted human ovarian fragments subjected to hypoxia. We showed that Z-VAD-FMK maintains the metabolic activity of granulosa cells, reduced HGL5 cell death, and decreased the cleavage of PARP protein in vitro.

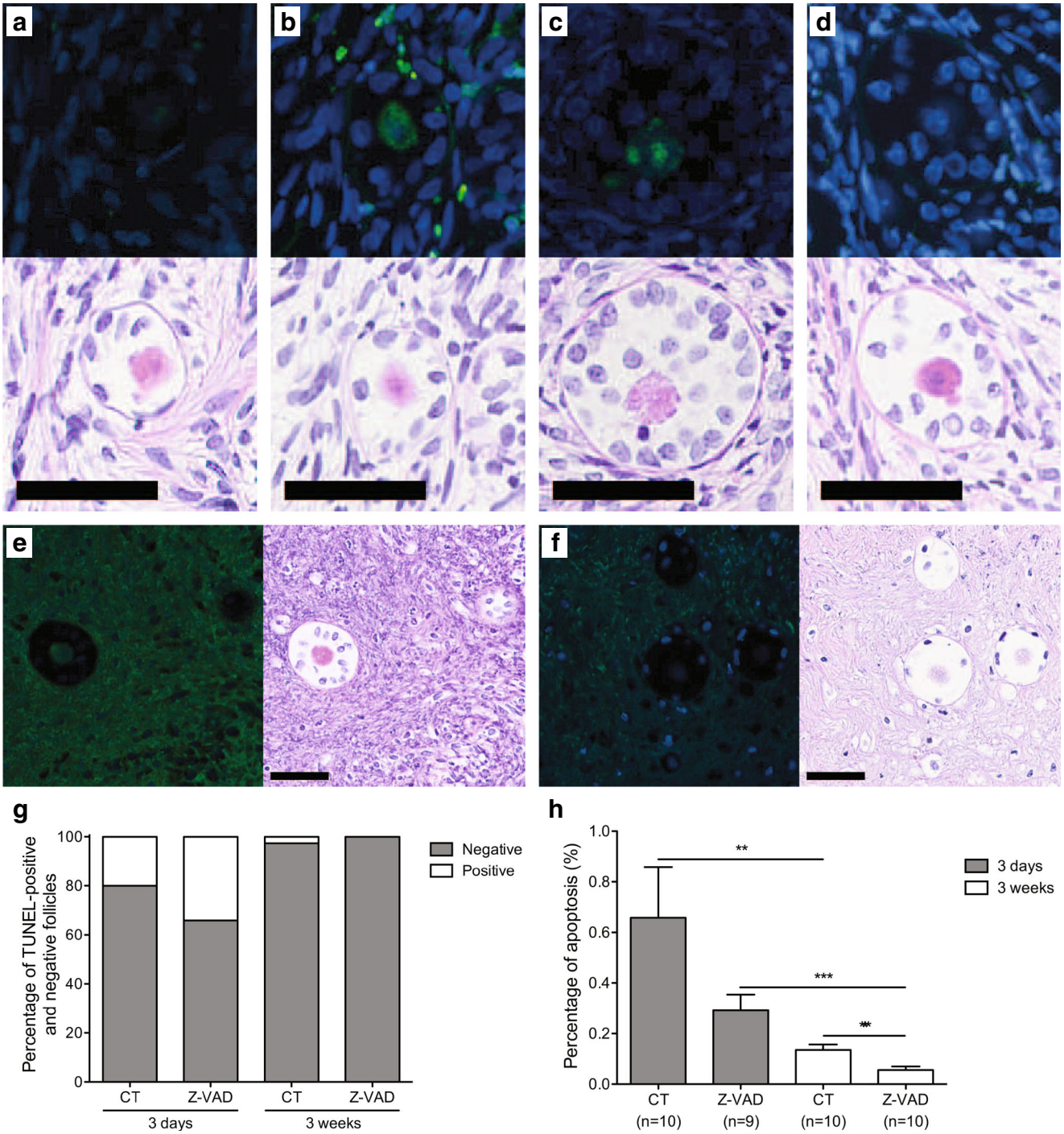


**Fig. 3** Representative images of follicular apoptosis and TUNEL staining quantification in ovarian tissue after transplantation. TUNEL-positive primordial (**a**), primary (**b**), and secondary (**c**) follicles and their corresponding H&E staining. TUNEL-negative morphologically abnormal follicle and corresponding H&E staining (**d**). TUNEL-positive (**e**) and negative (**f**) follicles in fibrotic area and corresponding H&E. Quantitative evaluation of the follicular apoptosis (**g**) and the percentage of TUNEL-positive staining per $mm^2$ throughout ovarian tissue (**h**). Scale bar: 50 μM. ** $P < 0.01$ and *** $P < 0.001$

Moreover, it slightly improves primary follicular preservation and reduces global apoptosis after 3 weeks of transplantation.

Follicular loss after ovarian tissue transplantation is one of the main cause of limited success rate of the procedure to restore fertility [36]. To optimize the function of the graft, quality improvement and follicular preservation of ovarian transplants have to be achieved. Within ovaries, the subtle balance between pro- and anti-apoptotic molecules largely controls the dynamics of follicle development [37]. Even though follicles survived to cryopreservation protocols [38], follicular apoptosis in frozen/thawed ovarian tissue has been demonstrated [13, 39–41]. Two previous studies also identified apoptotic follicles shortly after ovarian

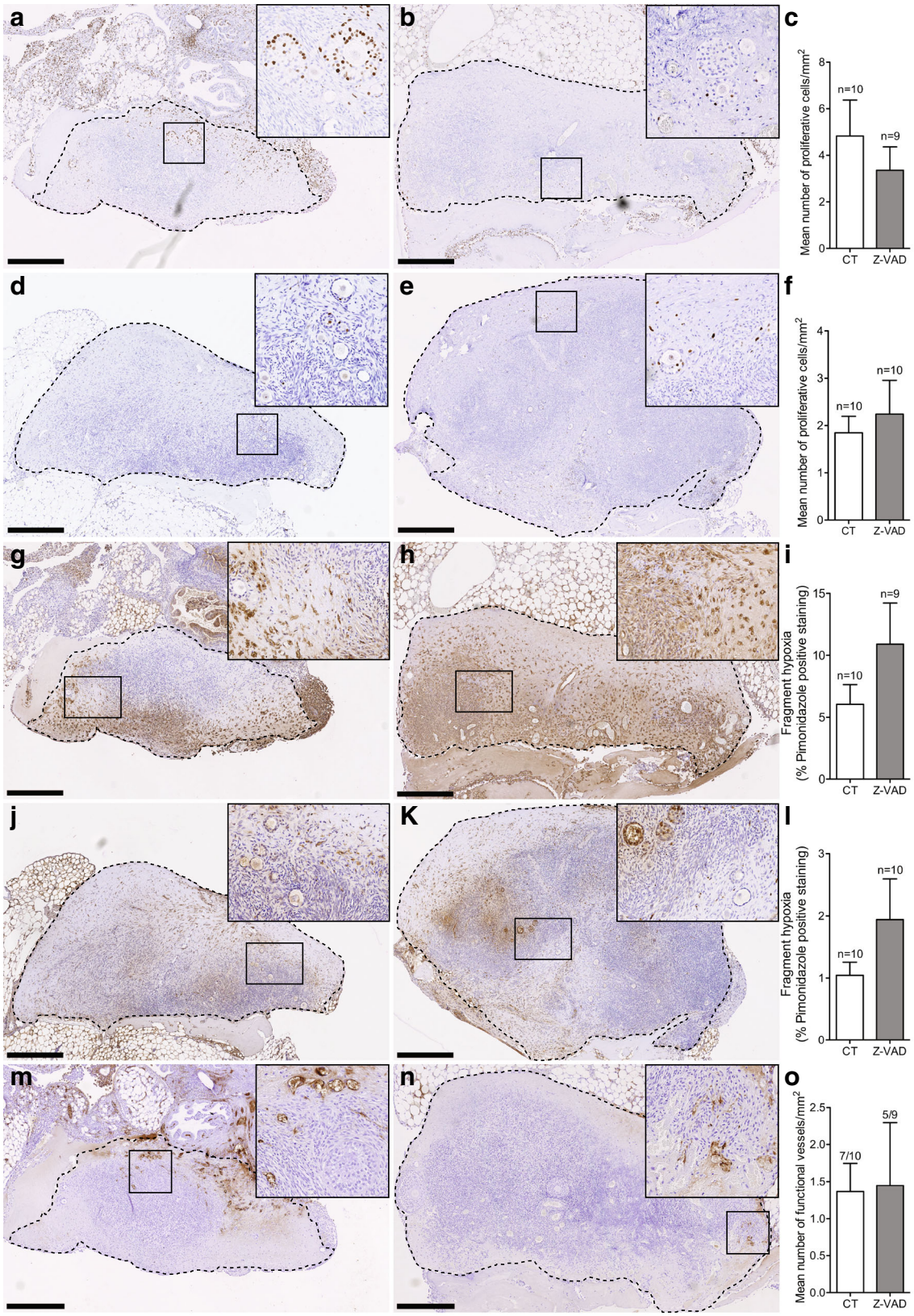


tissue transplantation [20, 21], revealing the importance of apoptosis after these processes. Caspases are the main effector molecules of apoptosis and all the pathways activating apoptosis converge towards these proteases [42]. The cleavage of caspase-

◀ **Fig. 4** Analysis of the proliferative status, hypoxia and functional vascular network of the ovarian tissue after grafting. Representative illustrations of proliferative cells from control (**a** and **d**, 3 days and 3 weeks respectively) and Z-VAD-FMK-treated grafts (**b** and **e**, 3 days and 3 weeks respectively). Quantitative assessment of the mean number of proliferative cells/mm$^2$ 3 days (**c**) or 3 weeks (**f**) after transplantation in SCID mice. Representative illustrations of hypoxic areas from control (**g** and **j**, 3 days and 3 weeks respectively) and Z-VAD-FMK-treated grafts (**h** and **k**, 3 days and 3 weeks respectively). Quantitative assessment of the percentage of pimonidazole positive staining 3 days (**i**) or 3 weeks (**l**) after transplantation in SCID mice. Representative illustrations of functional blood vessels from control (**m**) and Z-VAD-FMK-treated fragments (**n**) 3 days after grafting in SCID mice and the corresponding quantification (**o**). Scale bar: 500 μM

3 is therefore an important trigger for the execution of apoptosis. Caspase-3 activation was demonstrated in human ovaries after cryopreservation [13, 40] and Rahimi et al. suggested that caspase machinery is activated after xenograft [43]. This caspase activation is prevented by Z-VAD-FMK that improves the recovery and the survival of multiple cryopreserved cell types [44]. Therefore, it was hypothesized that Z-VAD-FMK supplementation could help to prevent follicular apoptosis occurring soon after ovarian tissue transplantation.

Our results obtained with HGL5 cells clearly indicated a protective effect of the Z-VAD-FMK against apoptosis in hypoxic conditions. To be closer to the in vivo situation, the same experiments were repeated with human granulosa cells isolated from follicular fluid but proliferation and viability of these cells were not affected by Z-VAD-FMK treatment. Indeed, hGC were found to be highly resistant to $CoCl_2$-induced apoptosis when evaluated by flow cytometry. However, PARP cleavage is prevented by Z-VAD-FMK under $CoCl_2$ treatment, suggesting that the anti-apoptotic effectively inhibits the activation of the caspases in those cells. When ovarian cortex was grafted in vivo with Z-VAD-FMK, no improvement of follicular pool and global tissue preservation was observed in fragments recovered 3-days post-grafting. Conversely, after 3 weeks of transplantation, the mean number of primary follicles detected in fragments treated with Z-VAD-FMK was higher than in the control ones. This improvement was associated with a decreased percentage of apoptosis in the tissue. If these results are encouraging, they are nonetheless surprising considering the short half-life of Z-VAD-FMK that is documented to be about 4 hours [45]. In addition, the relatively low amount of follicles and TUNEL-labeled tissue observed in the grafted fragments suggests that the biological significance of these results is questionable. They should therefore be interpreted cautiously. In a previous study, Liu et al. investigated DNA fragmentation as early as 2 hours after grafting and they observed a marked increase in the number of TUNEL-positive granulosa or stromal cells. Conversely, ovaries analyzed after 3 days of transplantation showed a low number of TUNNEL-positive cells [20].

The low level of apoptosis observed early after transplantation could also suggest that some other mechanisms are responsible for follicle loss following ovarian transplantation. To date, all the mechanisms involved have not yet been clearly elucidated.

Recently, an emerging theory focusing on the immediate follicular activation after grafting was proposed as a significant cause of follicle loss after ovarian tissue transplantation [46–48]. In our study, even if mice receiving the ovarian pieces were not ovariectomised, the proportion of growing follicles was increased as early as 3 days after xenograft compared to resting follicles (Online Resource 3). However, the proliferative activity of primordial follicles was not evaluated. As previously demonstrated, this result confirms that AMH is not sufficient to prevent follicular activation [49] and that other pathways are involved in the control of follicular recruitment after transplantation [48, 50].

At reperfusion phase, reactive oxygen species (ROS) are generated and could also be responsible of follicular loss. They accumulate in nutrient-deficient conditions and play an important role as an inducer of cell death pathways, including apoptosis but also necrosis and autophagy [19]. Necrosis has already been observed after ovarian tissue transplantation [51, 52], and targeting ischemic necrosis after this process has been proven beneficial [53]. The detrimental role of autophagy is directly linked to the duration of the ischemic period [19, 54] and it is mainly controlled by mTOR, which is inactivated in nutrient withdrawal or ROS accumulation conditions. Previous studies highlighted the importance of the mTOR signaling in the control of activation of primordial follicles for the maintenance of the length of female reproductive life [55]. McLaughlin et al. also suggested that oocyte loss occurring in cultured human cortical strips in response to mTOR inhibition could be attributed to autophagy [56].

Altogether, these data strengthen the hypothesis of likely coexistence of several regulatory pathways of follicular growth and multiple types of cell death governing follicular fate in case of ovarian tissue transplantation.

In summary, our in vitro results clearly indicate that Z-VAD-FMK is able to limit HGL5 cell death and partially reverse the PARP cleavage induced by $CoCl_2$ treatment. Inclusion of this caspase inhibitor in the collagen matrix during in vivo transplantation of ovarian cortex slightly improves primary follicular preservation and reduces global apoptosis after 3 weeks of transplantation. A combined approach targeting different cell death pathways and follicular activation should be considered. Nevertheless, if such treatments were to be considered for adaptation to human ovarian tissue transplantation, we should take care of its safety as germ cell DNA is inherited to offspring. We should remember that viability and functionality of the preserved oocytes are additional parameters that should always be examined. Rescuing follicles to improve the fertility potential of ovarian graft is essential but genetic material of germ cells must be intact.

**Acknowledgments** The authors thank the CPMA-CHR Citadelle Liège for their contribution to follicular fluids collection. The authors are very grateful to M. C. Masereel and S. Schoenen for their help for follicular quantification. The authors acknowledge M. Dehuy, E. Konradowski, E. Feyereisen, and I. Dasoul for their excellent technical assistance.

The authors thank the Fonds de la Recherche Scientifique-FNRS (F.R.S.-FNRS, Télévie, Belgium; 7.4597.12-7.4622.14-7.4590.16), the Fondation

contre le Cancer (foundation of public interest, Belgium), the Fonds spéciaux de la Recherche (University of Liège), the Centre Anticancéreux près l'Université de Liège, the Fonds Léon Fredericq (University of Liège), the Direction Générale Opérationnelle de l'Economie, de l'Emploi et de la Recherche from the Service Public de Wallonie (SPW, Belgium), the Interuniversity Attraction Poles Programme-Belgian Science Policy (Brussels, Belgium), the Plan National Cancer (Service Public Fédéral), and the Actions de Recherche Concertées (University of Liege, Belgium). The authors also thank the GIGA (Groupe Interdisciplinaire de Génoprotéomique Appliquée, University of Liege, Belgium) for the access to the GIGA-Imaging and Flow Cytometry platform and Dr. S. Ormenese and R. Stephan for their support with FACS analyses.

**Author's roles** MF performed experiments, interpreted data, and wrote the manuscript. LN contributed to in vitro experiments. LH and SL interpreted data and revised the manuscript. SB performed the computer images analysis. MN conceived and designed the study and corrected the manuscript. CM conceived and designed the study, interpreted data, corrected the manuscript, and substantially contributed to critical revisions. All authors read and approved the final manuscript.

## Compliance with ethical standards

**Ethical approval** All procedures performed in studies involving human participants were in accordance with the ethical standards of the institutional and/or national research committee and with the 1964 Helsinki declaration and its later amendments or comparable ethical standards.

All applicable international, national, and/or institutional guidelines for the care and use of animals were followed. All procedures performed in studies involving animals were in accordance with the ethical standards of the institution or practice at which the studies were conducted.

The use of human follicular fluid and ovarian tissue was approved by the Ethics Committee of the CHR Citadelle, University of Liège (CE412/1508 and CE412/1448, respectively). The use of the xenograft model was approved by the Animal Ethics Committee of the University of Liège (Reference 1304, October 2012).

**Informed consent** Informed consent was obtained from all individual participants included in the study.

**Conflict of interest** The authors declare that they have no conflict of interest.

## References

1. Oktay K, Sonmezer M. Chemotherapy and amenorrhea: risks and treatment options. Curr Opin Obstet Gynecol. 2008;20(4):408–15. https://doi.org/10.1097/GCO.0b013e328307ebad.
2. Demeestere I, Simon P, Emiliani S, Delbaere A, Englert Y. Orthotopic and heterotopic ovarian tissue transplantation. Hum Reprod Update. 2009;15(6):649–65. https://doi.org/10.1093/humupd/dmp021.
3. Demeestere I, Simon P, Dedeken L, Moffa F, Tsepelidis S, Brachet C, et al. Live birth after autograft of ovarian tissue cryopreserved during childhood. Hum Reprod. 2015;30(9):2107–9. https://doi.org/10.1093/humrep/dev128.
4. Jensen AK, Macklon KT, Fedder J, Ernst E, Humaidan P, Andersen CY. 86 successful births and 9 ongoing pregnancies worldwide in women transplanted with frozen-thawed ovarian tissue: focus on birth and perinatal outcome in 40 of these children. J Assist Reprod Genet. 2016;34:325–36. https://doi.org/10.1007/s10815-016-0843-9.
5. Donnez J, Dolmans MM. Fertility preservation in women. N Engl J Med. 2017;377(17):1657–65. https://doi.org/10.1056/NEJMra1614676.
6. Van Eyck AS, Jordan BF, Gallez B, Heilier JF, Van Langendonckt A, Donnez J. Electron paramagnetic resonance as a tool to evaluate human ovarian tissue reoxygenation after xenografting. Fertil Steril. 2009;92(1):374–81.
7. Nugent D, Newton H, Gallivan L, Gosden RG. Protective effect of vitamin E on ischaemia-reperfusion injury in ovarian grafts. J Reprod Fertil. 1998;114(2):341–6.
8. Nisolle M, Casanas-Roux F, Qu J, Motta P, Donnez J. Histologic and ultrastructural evaluation of fresh and frozen-thawed human ovarian xenografts in nude mice. Fertil Steril. 2000;74(1):122–9.
9. Camboni A, Martinez-Madrid B, Dolmans MM, Nottola S, Van Langendonckt A, Donnez J. Autotransplantation of frozen-thawed ovarian tissue in a young woman: ultrastructure and viability of grafted tissue. Fertil Steril. 2008;90(4):1215–8. https://doi.org/10.1016/j.fertnstert.2007.08.084.
10. Israely T, Nevo N, Harmelin A, Neeman M, Tsafriri A. Reducing ischaemic damage in rodent ovarian xenografts transplanted into granulation tissue. Hum Reprod. 2006;21(6):1368–79.
11. Abir R, Fisch B, Jessel S, Felz C, Ben Haroush A, Orvieto R. Improving posttransplantation survival of human ovarian tissue by treating the host and graft. Fertil Steril. 2011;95(4):1205–10.
12. Shikanov A, Zhang Z, Xu M, Smith RM, Rajan A, Woodruff TK, et al. Fibrin encapsulation and vascular endothelial growth factor delivery promotes ovarian graft survival in mice. Tissue Eng Part A. 2011;17(23–24):3095–104. https://doi.org/10.1089/ten.TEA.2011.0204.
13. Soleimani R, Heytens E, Oktay K. Enhancement of neoangiogenesis and follicle survival by sphingosine-1-phosphate in human ovarian tissue xenotransplants. PLoS One. 2011;6(4):e19475.
14. Labied S, Delforge Y, Munaut C, Blacher S, Colige A, Delcombel R, et al. Isoform 111 of vascular endothelial growth factor (VEGF111) improves angiogenesis of ovarian tissue xenotransplantation. Transplantation. 2013;95(3):426–33. https://doi.org/10.1097/TP.0b013e318279965c.
15. Commin L, Buff S, Rosset E, Galet C, Allard A, Bruyere P, et al. Follicle development in cryopreserved bitch ovarian tissue grafted to immunodeficient mouse. Reprod Fertil Dev. 2012;24(3):461–71. https://doi.org/10.1071/RD11166.
16. Wang L, Ying YF, Ouyang YL, Wang JF, Xu J. VEGF and bFGF increase survival of xenografted human ovarian tissue in an experimental rabbit model. J Assist Reprod Genet. 2013;30(10):1301–11. https://doi.org/10.1007/s10815-013-0043-9.
17. Henry L, Labied S, Fransolet M, Kirschvink N, Blacher S, Noel A, et al. Isoform 165 of vascular endothelial growth factor in collagen matrix improves ovine cryopreserved ovarian tissue revascularisation after xenotransplantation in mice. Reprod Biol Endocrinol. 2015;13:12. https://doi.org/10.1186/s12958-015-0015-2.
18. Langbeen A, Ginneken CV, Fransen E, Bosmans E, Leroy JL, Bols PE. Morphometrical analysis of preantral follicular survival of VEGF-treated bovine ovarian cortex tissue following xenotransplantation in an immune deficient mouse model. Anim Reprod Sci. 2016;168:73–85. https://doi.org/10.1016/j.anireprosci.2016.02.029.
19. Kalogeris T, Baines CP, Krenz M, Korthuis RJ. Cell biology of ischemia/reperfusion injury. Int Rev Cell Mol Biol. 2012;298:229–317. https://doi.org/10.1016/B978-0-12-394309-5.00006-7.
20. Liu J, Van der Elst J, Van den Broecke R, Dhont M. Early massive follicle loss and apoptosis in heterotopically grafted newborn mouse ovaries. Hum Reprod. 2002;17(3):605–11.
21. Yang H, Lee HH, Lee HC, Ko DS, Kim SS. Assessment of vascular endothelial growth factor expression and apoptosis in the ovarian graft: can exogenous gonadotropin promote angiogenesis after ovarian transplantation? Fertil Steril. 2008;90(4 Suppl):1550–8. https://doi.org/10.1016/j.fertnstert.2007.08.086.
22. Goldar S, Khaniani MS, Derakhshan SM, Baradaran B. Molecular mechanisms of apoptosis and roles in cancer development and treatment. Asian Pac J Cancer Prev. 2015;16(6):2129–44.

23. Yaoita H, Ogawa K, Maehara K, Maruyama Y. Attenuation of ischemia/reperfusion injury in rats by a caspase inhibitor. Circulation. 1998;97(3):276–81.
24. Himi T, Ishizaki Y, Murota S. A caspase inhibitor blocks ischaemia-induced delayed neuronal death in the gerbil. Eur J Neurosci. 1998;10(2):777–81.
25. Cursio R, Gugenheim J, Ricci JE, Crenesse D, Rostagno P, Maulon L, et al. Caspase inhibition protects from liver injury following ischemia and reperfusion in rats. Transpl Int. 2000;13(Suppl 1):S568–72.
26. Iwata A, Harlan JM, Vedder NB, Winn RK. The caspase inhibitor z-VAD is more effective than CD18 adhesion blockade in reducing muscle ischemia-reperfusion injury: implication for clinical trials. Blood. 2002;100(6):2077–80. https://doi.org/10.1182/blood-2002-03-0752.
27. Azuara D, Sola A, Hotter G, Calatayud L, de Oca J. Apoptosis inhibition plays a greater role than necrosis inhibition in decreasing bacterial translocation in experimental intestinal transplantation. Surgery. 2005;137(1):85–91. https://doi.org/10.1016/j.surg.2004.06.008.
28. Emamaullee JA, Stanton L, Schur C, Shapiro AM. Caspase inhibitor therapy enhances marginal mass islet graft survival and preserves long-term function in islet transplantation. Diabetes. 2007;56(5):1289–98. https://doi.org/10.2337/db06-1653.
29. Slee EA, Zhu H, Chow SC, MacFarlane M, Nicholson DW, Cohen GM. Benzyloxycarbonyl-Val-Ala-Asp (OMe) fluoromethylketone (Z-VAD.FMK) inhibits apoptosis by blocking the processing of CPP32. Biochem J. 1996;315(Pt 1):21–4.
30. Henry L, Fransolet M, Labied S, Blacher S, Masereel MC, Foidart JM, et al. Supplementation of transport and freezing media with anti-apoptotic drugs improves ovarian cortex survival. J Ovarian Res. 2016;9(1):4. https://doi.org/10.1186/s13048-016-0216-0.
31. Zhang JM, Li LX, Yang YX, Liu XL, Wan XP. Is caspase inhibition a valid therapeutic strategy in cryopreservation of ovarian tissue? J Assist Reprod Genet. 2009;26(7):415–20. https://doi.org/10.1007/s10815-009-9331-9.
32. Shi FT, Cheung AP, Leung PC. Growth differentiation factor 9 enhances activin a-induced inhibin B production in human granulosa cells. Endocrinology. 2009;150(8):3540–6. https://doi.org/10.1210/en.2009-0267.
33. Fransolet M, Henry L, Labied S, Noël A, Nisolle M, Munaut C. In vitro evaluation of the anti-apoptotic drug Z-VAD-FMK on human ovarian granulosa cell lines for further use in ovarian tissue transplantation. J Assist Reprod Genet. 2015;32(10):1551–9. https://doi.org/10.1007/s10815-015-0536-9.
34. Gosden RG, Baird DT, Wade JC, Webb R. Restoration of fertility to oophorectomized sheep by ovarian autografts stored at −196 degrees C. Hum Reprod. 1994;9(4):597–603.
35. Fransolet M, Henry L, Labied S, Masereel MC, Blacher S, Noel A, et al. Influence of mouse strain on ovarian tissue recovery after engraftment with angiogenic factor. J Ovarian Res. 2015;8(1):14. https://doi.org/10.1186/s13048-015-0142-6.
36. Aubard Y, Piver P, Cogni Y, Fermeaux V, Poulin N, Driancourt MA. Orthotopic and heterotopic autografts of frozen-thawed ovarian cortex in sheep. Hum Reprod. 1999;14(8):2149–54.
37. Tilly JL, Kolesnick RN. Sphingolipids, apoptosis, cancer treatments and the ovary: investigating a crime against female fertility. Biochim Biophys Acta. 2002;1585(2–3):135–8.
38. Baird DT, Webb R, Campbell BK, Harkness LM, Gosden RG. Long-term ovarian function in sheep after ovariectomy and transplantation of autografts stored at −196 C. Endocrinology. 1999;140(1):462–71. https://doi.org/10.1210/en.140.1.462.
39. Rimon E, Cohen T, Dantes A, Hirsh L, Amit A, Lessing JB, et al. Apoptosis in cryopreserved human ovarian tissue obtained from cancer patients: a tool for evaluating cryopreservation utility. Int J Oncol. 2005;27(2):345–53.
40. Fauque P, Ben Amor A, Joanne C, Agnani G, Bresson JL, Roux C. Use of trypan blue staining to assess the quality of ovarian cryopreservation. Fertil Steril. 2007;87(5):1200–7. https://doi.org/10.1016/j.fertnstert.2006.08.115.
41. Xiao Z, Wang Y, Li L, Li SW. Cryopreservation of the human ovarian tissue induces the expression of Fas system in morphologically normal primordial follicles. Cryo Letters. 2010;31(2):112–9.
42. Hussein MR. Apoptosis in the ovary: molecular mechanisms. Hum Reprod Update. 2005;11(2):162–77. https://doi.org/10.1093/humupd/dmi001.
43. Isachenko V, Mallmann P, Petrunkina AM, Rahimi G, Nawroth F, Hancke K, et al. Comparison of in vitro- and chorioallantoic membrane (CAM)-culture systems for cryopreserved medulla-contained human ovarian tissue. PLoS One. 2012;7(3):e32549. https://doi.org/10.1371/journal.pone.0032549.
44. Stroh C, Cassens U, Samraj AK, Sibrowski W, Schulze-Osthoff K, Los M. The role of caspases in cryoinjury: caspase inhibition strongly improves the recovery of cryopreserved hematopoietic and other cells. FASEB J. 2002;16(12):1651–3. https://doi.org/10.1096/fj.02-0034fje.
45. Gururajan R, Lahti JM, Kidd VJ. Molecular analysis of programmed cell death in mammals. In: Adolph KW, editor. Human genome methods. New York, CRC Press; 1998. p. 135–157.
46. Roness H, Gavish Z, Cohen Y, Meirow D. Ovarian follicle burnout: a universal phenomenon? Cell Cycle. 2013;12(20):3245–6. https://doi.org/10.4161/cc.26358.
47. Silber S. Ovarian tissue cryopreservation and transplantation: scientific implications. J Assist Reprod Genet. 2016;33:1595–603. https://doi.org/10.1007/s10815-016-0814-1.
48. Gavish Z, Spector I, Peer G, Schlatt S, Wistuba J, Roness H, et al. Follicle activation is a significant and immediate cause of follicle loss after ovarian tissue transplantation. J Assist Reprod Genet. 2017;35:61–9. https://doi.org/10.1007/s10815-017-1079-z.
49. Kong HS, Kim SK, Lee J, Youm HW, Lee JR, Suh CS, et al. Effect of exogenous anti-Mullerian hormone treatment on cryopreserved and transplanted mouse ovaries. Reprod Sci. 2016;23(1):51–60. https://doi.org/10.1177/1933719115594021.
50. Ayuandari S, Winkler-Crepaz K, Paulitsch M, Wagner C, Zavadil C, Manzl C, et al. Follicular growth after xenotransplantation of cryopreserved/thawed human ovarian tissue in SCID mice: dynamics and molecular aspects. J Assist Reprod Genet. 2016;33:1585–93. https://doi.org/10.1007/s10815-016-0769-2.
51. Hancke K, Walker E, Strauch O, Gobel H, Hanjalic-Beck A, Denschlag D. Ovarian transplantation for fertility preservation in a sheep model: can follicle loss be prevented by antiapoptotic sphingosine-1-phosphate administration? Gynecol Endocrinol. 2009;25(12):839–43. https://doi.org/10.3109/09513590903159524.
52. Martinez-Madrid B, Donnez J, Van Eyck AS, Veiga-Lopez A, Dolmans MM, Van Langendonckt A. Chick embryo chorioallantoic membrane (CAM) model: a useful tool to study short-term transplantation of cryopreserved human ovarian tissue. Fertil Steril. 2009;91(1):285–92. https://doi.org/10.1016/j.fertnstert.2007.11.026.
53. Lee JR, Youm HW, Kim SK, Jee BC, Suh CS, Kim SH. Effect of necrostatin on mouse ovarian cryopreservation and transplantation. Eur J Obstet Gynecol Reprod Biol. 2014;178:16–20. https://doi.org/10.1016/j.ejogrb.2014.04.040.
54. Gong JS, Kim GJ. The role of autophagy in the placenta as a regulator of cell death. Clin Exp Reprod Med. 2014;41(3):97–107. https://doi.org/10.5653/cerm.2014.41.3.97.
55. Adhikari D, Liu K. mTOR signaling in the control of activation of primordial follicles. Cell Cycle. 2010;9(9):1673–4. https://doi.org/10.4161/cc.9.9.11626.
56. McLaughlin M, Patrizio P, Kayisli U, Luk J, Thomson TC, Anderson RA, et al. mTOR kinase inhibition results in oocyte loss characterized by empty follicles in human ovarian cortical strips cultured in vitro. Fertil Steril. 2011;96(5):1154–9 e1. https://doi.org/10.1016/j.fertnstert.2011.08.040.